
Tropical Expressivity of Neural Networks

Anonymous Author(s)

Affiliation

Address

email

Abstract

1 We propose an algebraic geometric framework to study the expressivity of linear
2 activation neural networks. A particular quantity that has been actively studied in
3 the field of deep learning is the number of linear regions, which gives an estimate
4 of the information capacity of the architecture. To study and evaluate information
5 capacity and expressivity, we work in the setting of tropical geometry—a combi-
6 natorial and polyhedral variant of algebraic geometry—where there are known
7 connections between tropical rational maps and feedforward neural networks. Our
8 work builds on and expands this connection to capitalize on the rich theory of
9 tropical geometry to characterize and study various architectural aspects of neural
10 networks. Our contributions are threefold: we provide a novel tropical geometric
11 approach to selecting sampling domains among linear regions; an algebraic result
12 allowing for a guided restriction of the sampling domain for network architectures
13 with symmetries; and an open source library to analyze neural networks as tropical
14 Puiseux rational maps. We provide a comprehensive set of proof-of-concept nu-
15 merical experiments demonstrating the breadth of neural network architectures to
16 which tropical geometric theory can be applied to reveal insights on expressivity
17 characteristics of a network. Our work provides the foundations for the adaptation
18 of both theory and existing software from computational tropical geometry and
19 symbolic computation to deep learning.

20 1 Introduction

21 Deep learning has become the undisputed state-of-the-art for data analysis and has wide-reaching
22 prominence in many fields of computer science, despite still being based on a limited theoretical
23 foundation. Developing theoretical foundations to better understand the unparalleled success of deep
24 neural networks is one of the most active areas of research in modern statistical learning theory.
25 *Expressivity* is one of the most important approaches to quantifiably measuring the performance of a
26 deep neural network—such as how they are able to represent highly complex information implicitly
27 in their weights and to generalize from data—and therefore key to understanding the success of deep
28 learning.

29 *Tropical geometry* is a reinterpretation of algebraic geometry that features piecewise linear and
30 polyhedral constructions, where combinatorics naturally comes into play [e.g., 1, 2, 3]. These
31 characteristics of tropical geometry make it a natural framework for studying the linear regions in a
32 neural network—an important quantity in deep learning representing the network information capacity
33 [4, 5, 6, 7, 8, 9, 10]. The intersection of deep learning theory and tropical geometry is a relatively
34 new area of research with great potential towards the ultimate goal of understanding how and why
35 deep neural networks perform so well. In this paper, we propose a new perspective for measuring
36 and estimating the expressivity and information capacity of a neural networks by developing and
37 expanding known connections between neural networks and tropical rational functions in both theory
38 and practice.

39 **Related Work.** Tropical geometry has been used to characterize deep neural networks with piece-
 40 wise linear activation functions, including two of the most popular and widely-used activation
 41 functions, namely, rectified linear units (ReLU) and maxout units. The first explicit connection
 42 between tropical geometry and neural networks establishes that the decision boundary of a deep
 43 neural network with ReLU activation functions is a tropical rational function [11]. Concurrently,
 44 it was established that the maxout activation function fits input data by a tropical polynomial [12].
 45 These works considered neural networks whose input domain is Euclidean, which was recently
 46 developed to incorporate tropically-motivated input domains, in particular, the tropical projective
 47 torus [13]. Most recently, tropical geometry has been used to construct convolutional neural networks
 48 that are robust to adversarial attacks via tropical decision boundaries [14].

49 **Contributions.** In this paper, we establish novel algebraic and geometric tools to quantify the
 50 expressivity of a neural network. Networks with a piecewise linear activation compute piecewise
 51 linear functions where the input space is divided into areas; the network computing a single linear
 52 function on each area. These areas are referred to as the *linear regions* of the network; the number
 53 of distinct linear regions is a quantifiable measure of expressivity of the network [e.g., 5]. In our
 54 work, we not only study the number of linear regions, we aim to understand their *geometry*. The main
 55 contributions of our work are the following.

- 56 • We provide a geometric characterization of the linear regions in a neural network via the
 57 input space: estimating the linear regions is typically carried out by random sampling from
 58 the input space, where randomness may cause some linear regions of a neural network to be
 59 missed and result in an inaccurate information capacity measure. We propose an *effective*
 60 *sampling domain* as a ball of radius R , which is a subset of the entire sampling space that
 61 hits all of the linear regions of a given neural network. We compute bounds for the radius R
 62 based on a combinatorial invariant known as the *Hoffman constant*, which effectively gives
 63 a geometric characterization and guarantee for the linear regions of a neural network.
- 64 • We exploit geometric insight into the linear regions of a neural network to gain dramatic
 65 computational efficiency: when networks exhibit invariance under symmetry, we can restrict
 66 the sampling domain to a *fundamental domain* of the group action and thus reduce the
 67 number of samples required. We experimentally demonstrate that sampling from the
 68 fundamental domain provides an accurate estimate of the number of linear regions with a
 69 fraction of the compute requirements.
- 70 • We provide an open source library integrated into the Open Source Computer Algebra
 71 Research (OSCAR) system [15] which converts both trained and untrained arbitrary neural
 72 networks into algebraic symbolic objects. This contribution then opens the door for the
 73 extensive theory and existing software on symbolic computation and computational tropical
 74 geometry to be used to study neural networks.

75 The remainder of this paper is organized as follows. We provide an overview of the technical
 76 background on tropical geometry and its connection to neural networks in Section 2. We then devote
 77 a section to each of the contributions listed above—Sections 3, 4, and 5, respectively—in which we
 78 present our theoretical contributions and numerical experiments. We close the paper with a discussion
 79 on limitations of our work and directions for future research in Section 6.

80 2 Technical Background

81 In this section, we give basic definitions from tropical geometry required to write tropical expressions
 82 for neural networks.

83 2.1 Tropical Polynomials

84 Algebraic geometry studies geometric properties of solution sets of polynomial systems that can
 85 be expressed algebraically, such as their degree, dimension, and irreducible components. *Tropical*
 86 *geometry* is a variant of algebraic geometry where the polynomials are defined in the *tropical semiring*,
 87 $\mathbb{R} = (\mathbb{R} \cup \{\infty\}, \oplus, \odot)$ where the addition and multiplication operators are given by $a \oplus b = \max(a, b)$
 88 and $a \odot b = a + b$, respectively. Define $a \oslash b := a - b$.

89 Using these operations, we can write polynomials as $\bigoplus_m a_m T^m$, where a_i are coefficients, $T \in \bar{\mathbb{R}}$,
 90 and where the sum is indexed by a finite subset of \mathbb{N}^n . In our work, we consider the following
 91 generalizations of tropical polynomials.

92 **Definition 2.1.** A *tropical Puiseux polynomial* in the indeterminates T_1, \dots, T_n is a formal expression
 93 of the form $\bigoplus_m a_m T^m$ where the index n runs through a finite subset of $\mathbb{Q}_{\geq 0}^m$ and $T^m = T_1^{m_1} \odot$
 94 $\dots \odot T_n^{m_n}$, and taking powers in the tropical sense.

95 **Definition 2.2.** A *tropical Puiseux rational map* in T_1, \dots, T_n is a tropical quotient of the form $p \oslash q$
 96 where p, q are tropical Puiseux polynomials.

97 Tropical (Puiseux) polynomials and rational maps induce functions from $\mathbb{R}^n \rightarrow \mathbb{R}$, which take a point
 98 $x \in \mathbb{R}^n$ to the number obtained by substituting $T = x$ in the algebraic expression and performing the
 99 (tropical) operations. It is important to note that tropically, the formal algebraic expression contains
 100 strictly more information than the corresponding function, since different tropical expressions can
 101 induce the same function.

102 2.2 Tropical Expressions for Neural Networks

103 We now overview and recast the framework of [11], which establishes the first explicit connection
 104 between tropical geometry and neural networks, in a slightly different language for our results.

105 As in [11], the neural networks we will focus on are fully connected multilayer perceptrons with ReLU
 106 activation, i.e., functions $\mathbb{R}^n \rightarrow \mathbb{R}^m$ of the form $\sigma \circ L_d \circ \sigma \circ L_{i-1} \circ \dots \circ L_1$ where $L_i : \mathbb{R}^{n_{i-1}} \rightarrow \mathbb{R}^{n_i}$
 107 is an affine map and $\sigma(t) = \max\{t, 0\}$. For the remainder of this paper, we use the term “neural
 108 network” to refer solely to these. We will always assume that the weights and biases of our neural
 109 networks are rational numbers. From a computational perspective, this is not a serious restriction
 110 since this is sufficient to describe any neural network with weights and biases given by floating point
 111 numbers. We refer to the tuple $[n, n_1, \dots, n_{d-1}, m]$ as the *architecture* of the neural network.

112 One of the key observations intersecting tropical geometry and deep learning is that, up to rescaling
 113 of rational weights to obtain integers, neural networks can be written as tropical rational functions
 114 [11, Theorem 5.2]. From a more computational perspective, it is usually preferable to avoid such
 115 rescaling and simply work with the original weights. The proof of Theorem 5.2 in [11] can directly
 116 be adapted to show that any neural network can be written as the function associated to a tropical
 117 Puiseux rational map. In their language, this corresponds to saying that any neural network is a
 118 *tropical rational signomial* with nonnegative rational exponents.

119 3 Sampling Domain Selection Using a Hoffman Constant

120 Estimating the number of linear regions of a neural network typically proceeds by sampling points
 121 from the input domain and counting the memberships of these points. To guarantee that membership
 122 is exhaustive, we seek a sampling domain as a sufficiently large ball so that all linear regions are
 123 intersected. At the same time, we would like for the ball to be as small as possible to guarantee
 124 efficient sampling. We are thus searching for the smallest ball from which we can sample in such a
 125 way that all linear regions are intersected. Given the polyhedral geometry of tropical Puiseux rational
 126 maps, it turns out that the radius of this smallest ball that we seek is closely related to the *Hoffman*
 127 *constant*, which is a combinatorial invariant.

128 Our contribution in this section is a definition of a Hoffman constant of a neural network; we
 129 demonstrate its relationship to the smallest sampling ball and propose algorithms to compute its true
 130 value and lower and upper bounds.

131 3.1 Defining a Neural Network Hoffman Constant

132 In simpler terms, the Hoffman constant can be expressed for a matrix as follows. Let A be an $m \times n$
 133 matrix. For any $b \in \mathbb{R}^m$, let $P(A, b) = \{x \in \mathbb{R}^n : Ax \leq b\}$ denote the polyhedron determined by
 134 A and b . For a nonempty polyhedron $P(A, b)$, let $d(u, P(A, b)) = \min\{\|u - x\| : x \in P(A, b)\}$
 135 denote the distance from a point $u \in \mathbb{R}^n$ to the polyhedron, measured under an arbitrary norm $\|\cdot\|$

136 on \mathbb{R}^n . Then there exists a constant $H(A)$ only depending on A such that

$$d(u, P_{A,b}) \leq H(A) \|(Au - b)_+\| \quad (1)$$

137 where $x_+ = \max\{x, 0\}$ is applied coordinate-wise [16]. The constant $H(A)$ is called the *Hoffman*
138 *constant* of A .

139 **The Hoffman Constant for Tropical Polynomials and Rational Functions.** Let $f : \mathbb{R}^n \rightarrow \mathbb{R}$
140 be a tropical Puiseux polynomial and let $\mathcal{U} = \{U_1, \dots, U_m\}$ be the set of linear regions of f . Let
141 $f(x) = a_{i_1}x_1 + \dots + a_{i_n}x_n + b_i$ occur on the region U_i . Further, let $A = [a_{ij}]_{m \times n}$ be the matrix of
142 coefficients in the expression of f over \mathcal{U} . The linear region U_i is defined by the following inequalities

$$a_{i_1}x_1 + \dots + a_{i_n}x_n + b_i \geq a_{j_1}x_1 + \dots + a_{j_n}x_n + b_j, \quad \forall j = 1, 2, \dots, m. \quad (2)$$

143 In matrix form, (2) is equivalent to

$$(A - \mathbf{1}a_i)x \leq b_i\mathbf{1} - b \quad (3)$$

144 where $\mathbf{1}$ is a column vector of all 1's; a_i is the i th row vector of A ; and b is a column vector of all
145 b_i . Denote $\tilde{A}_{U_i} := A - \mathbf{1}a_i$ and $\tilde{b}_{U_i} := b_i\mathbf{1} - b$. Then the linear region U_i is captured by the linear
146 system of inequalities $\tilde{A}_{U_i}x \leq \tilde{b}_{U_i}$.

147 **Definition 3.1.** Let $f : \mathbb{R}^n \rightarrow \mathbb{R}$ be a tropical Puiseux polynomial. The *Hoffman constant* of f is
148 defined as

$$H(f) = \max_{U_i \in \mathcal{U}} H(\tilde{A}_{U_i}).$$

149 Care needs to be taken in defining a Hoffman constant for a tropical Puiseux rational map: We want
150 to avoid having all linear regions defined by systems of linear inequalities, since there exist linear
151 regions which are not convex. To do so, we consider convex refinements of linear regions induced by
152 intersections of linear regions of tropical polynomials.

153 **Definition 3.2.** Let $p \oslash q$ be a difference of two tropical Puiseux polynomials. Let A_p (respectively
154 A_q) be the $m_p \times n$ (respectively $m_q \times n$) matrix of coefficients for p (respectively q). The *Hoffman*
155 *constant* of $p \oslash q$ is

$$H(p \oslash q) := \max \left\{ H \left(\begin{bmatrix} A_p \\ A_q \end{bmatrix} - \mathbf{1} \begin{bmatrix} a_{i_p} \\ a_{i_q} \end{bmatrix} \right) : i_p = 1, \dots, m_p; i_q = 1, \dots, m_q \right\}. \quad (4)$$

156 Let f be a tropical Puiseux rational map. Then the *Hoffman constant* of f is defined as the minimal
157 Hoffman constant of $H(p \oslash q)$ over all possible expressions of $f = p \oslash q$.

158 Given the correspondence between neural networks and tropical Puiseux rational maps, the Hoffman
159 constant is well-defined for any neural network and may be computed from the geometry and
160 combinatorics of its linear regions.

161 3.2 The Minimal Effective Radius

162 For a neural network whose tropical Puiseux rational map is $f : \mathbb{R}^n \rightarrow \mathbb{R}$, let $\mathcal{U} = \{U_1, \dots, U_m\}$ be
163 the collection of all linear regions. For any $x \in \mathbb{R}^n$, define the *minimal effective radius* of f at x as

$$R_f(x) := \min\{r : B(x, r) \cap U_i \neq \emptyset, U_i \in \mathcal{U}\}$$

164 where $B(x, r)$ is the ball of radius r centered at x . That is, $R_f(x)$ is the minimal radius such that the
165 ball $B(x, r)$ intersects all linear regions. It is the smallest required radius of sampling around x in
166 order to express the full classifying capacity of the neural network f .

167 We start with the following lemma which relates the minimal effective radius to the Hoffman constant
168 when f is a tropical Puiseux polynomial.

169 **Lemma 3.3.** Let f be a tropical Puiseux polynomial and $x \in \mathbb{R}^n$ be any point, then

$$R_f(x) \leq H(f) \max_{U_i \in \mathcal{U}} \|(\tilde{A}_{U_i}x - \tilde{b}_{U_i})_+\|. \quad (5)$$

170 In particular, we are interested in studying when \mathbb{R}^m and \mathbb{R}^n are equipped with the ∞ -norm. In
 171 this case, the minimal effective radius can be related to the Hoffman constant and function value
 172 of $f = p \oslash q$. For a tropical Puiseux polynomial $p(x) = \max_{1 \leq i \leq m_p} \{a_i x + b_i\}$, let $\check{p}(x) =$
 173 $\min_{1 \leq j \leq m_q} \{a_j x + b_j\}$ be its min-conjugate.

174 **Proposition 3.4.** *Let $f = p \oslash q$ be a tropical Puiseux rational map. For any $x \in \mathbb{R}^n$, we have*

$$R_f(x) \leq H(p \oslash q) \max\{p(x) - \check{p}(x), q(x) - \check{q}(x)\}. \quad (6)$$

175 3.3 Computing and Estimating Hoffman Constants

176 **The PVZ Algorithm.** In [17], the authors proposed a combinatorial algorithm to compute the
 177 precise value of the Hoffman constant for a matrix $A \in \mathbb{R}^{m \times n}$, which we refer to as the *Peña–Vera–*
 178 *Zuluaga (PVZ) algorithm* and sketch its main steps here.

179 **Definition 3.5.** A set-valued map $\Phi : \mathbb{R}^n \rightarrow \mathbb{R}^m$ assigns a set $\Phi(x) \subseteq \mathbb{R}^m$. The map is surjective
 180 if $\Phi(\mathbb{R}^n) = \cup_x \Phi(x) = \mathbb{R}^m$. Let $A \in \mathbb{R}^{m \times n}$. For any $J \subseteq \{1, 2, \dots, m\}$, let A_J be the submatrix
 181 of A consisting of rows with indices in J . The set J is called *A-surjective* if the set-valued map
 182 $\Phi(x) = A_J x + \{y \in \mathbb{R}^J : y \geq 0\}$ is surjective.

183 Notice that *A-surjectivity* is a generalization of linear independence of row vectors. We illustrate this
 184 observation in the following two examples.

185 **Example 3.6.** If J is such that A_J is full-rank, then J is *A-surjective*, since for any $y \in \mathbb{R}^J$, there
 186 exists $x \in \mathbb{R}^n$ such that $y = A_J x$.

187 **Example 3.7.** Let $A = \mathbf{1}_{m \times n}$ be the $m \times n$ matrix whose entries are 1's. For any subset J of
 188 $\{1, \dots, m\}$ and for any $y \in \mathbb{R}^J$, let $x \in \mathbb{R}^n$ such that $\sum_i x_i \leq \min\{y_j, j \in J\}$. Then $y - A_J x \geq 0$.
 189 Thus any J is *A-surjective*.

190 The PVZ algorithm is based on the following characterization of Hoffman constant.

191 **Proposition 3.8.** [17, Proposition 2] *Let $A \in \mathbb{R}^{m \times n}$. Equip \mathbb{R}^m and \mathbb{R}^n with norm $\|\cdot\|$ and denote
 192 its dual norm by $\|\cdot\|^*$. Let $\mathcal{S}(A)$ be the set of all *A-surjective* sets. Then*

$$H(A) = \max_{J \in \mathcal{S}(A)} H_J(A) \quad (7)$$

193 *where*

$$H_J(A) = \max_{y \in \mathbb{R}^m, \|y\| \leq 1} \min_{\substack{x \in \mathbb{R}^n \\ A_J x \leq y_J}} \|x\| = \frac{1}{\min_{v \in \mathbb{R}_+^J, \|v\|^* = 1} \|A_J^\top v\|^*}. \quad (8)$$

194 This characterization is particularly useful when \mathbb{R}^m and \mathbb{R}^n are equipped with the ∞ -norm, since
 195 the computation of (8) reduces to a linear programming (LP) problem. The key problem is how to
 196 maximize over all *A-surjective* sets. To do this, the PVZ algorithm maintains three collections of
 197 sets \mathcal{F} , \mathcal{I} , and \mathcal{J} where during every iteration: (i) \mathcal{F} contains J such that J is *A-surjective*; (ii) \mathcal{I}
 198 contains J such that J is not *A-surjective*; and (iii) \mathcal{J} contains candidates J whose *A-surjectivity*
 199 will be tested.

200 To detect whether a candidate $J \in \mathcal{J}$ is surjective, the PVZ algorithm requires solving

$$\min \|A_J^\top v\|_1, \text{ s.t. } v \in \mathbb{R}_+^J, \|v\|_1 = 1. \quad (9)$$

201 If the optimal value is positive, then J is *A-surjective*, and J is assigned to \mathcal{F} and all subsets of J are
 202 removed from \mathcal{J} . Otherwise, the optimal value is 0 and there is $v \in \mathbb{R}_+^J$ such that $A_J^\top v = 0$. Let
 203 $I(v) = \{i \in J : v_i > 0\}$ and assign $I(v)$ to \mathcal{I} . Let $\hat{J} \in \mathcal{J}$ be any set containing $I(v)$. Replace all
 204 such \hat{J} by sets $\hat{J} \setminus \{i\}, i \in I(v)$ which are not contained in any sets in \mathcal{F} . The implementation used in
 205 our paper directly uses the MATLAB code provided by [17].

206 **Lower and Upper Bounds.** A limitation of the PVZ algorithm is that during each loop, every set in
 207 \mathcal{J} needs to be tested, and each test requires solving a LP problem. Although solving one LP problem
 208 in practice is fast, a complete while loop calls the LP solver many times.

209 Here, we propose an algorithm to estimate lower and upper bounds for Hoffman constants. An
 210 intuitive way to estimate the lower bound is to sample a number of random subsets from $\{1, \dots, m\}$
 211 and test for A -surjectivity. This method bypasses optimizing combinatorially over $\mathcal{S}(A)$ of A -
 212 surjective sets and gives a lower bound of Hoffman constant by Proposition 3.8.

213 To get an upper of Hoffman constant, we use the result from [18].

214 **Theorem 3.9.** [18, Theorem 4.2] Let $A \in \mathbb{R}^{m \times n}$. Let $\mathcal{D}(A)$ be a set of subsets of $J \subseteq \{1, \dots, m\}$
 215 such that A_J is full rank. Let $\mathcal{D}^*(A)$ be the set of maximal elements in $\mathcal{D}(A)$. Then the Hoffman
 216 constant measured under 2-norm is bounded by

$$H(A) \leq \max_{J \in \mathcal{D}^*(A)} \frac{1}{\hat{\rho}(A_J)} \quad (10)$$

217 where $\hat{\rho}(A)$ is the smallest singular value of A .

218 Using the fact that $\|\cdot\|_1 \geq \|\cdot\|_2$, and the characterization from (8), we see that the upper bound also
 219 holds when \mathbb{R}^m and \mathbb{R}^n are equipped with the ∞ -norm. However, enumerating all maximal elements
 220 in $\mathcal{D}(A)$ is not an improvement over enumerating A -surjective sets from a computational perspective.
 221 Instead, we will retain the strategy as in lower bound estimation to sample a number of sets from
 222 $\{1, 2, \dots, m\}$ and approximate the upper bound by (10). We verify this approach via synthetic data.
 223 The experiments are relegated to the Appendix.

224 4 Symmetry and the Fundamental Domain

225 In this section, we study a geometric characterization of the sampling domain for networks exhibiting
 226 symmetry. This corresponds to *invariant neural networks*.

227 4.1 Linear Regions of Invariant Neural Networks

228 The notion of invariance for a neural network describes when a manipulation of the input domain
 229 does not affect the output of the network. The manipulations we consider here are group actions.

230 **Definition 4.1.** Let $\sigma : \mathbb{R}^n \rightarrow \mathbb{R}$ be a piecewise linear function, and let G be a group acting on the
 231 domain \mathbb{R}^n . σ is *invariant* under the group action of G if for any element $g \in G$, $\sigma \circ g = \sigma$.

232 Given an invariant neural network, we can then define a sampling domain that takes into account the
 233 effect of the group action.

234 **Definition 4.2.** Let G be a group acting on \mathbb{R}^n . A subset $\Delta \subseteq \mathbb{R}^n$ is a *fundamental domain* if it
 235 satisfies two following conditions: (i) $\mathbb{R}^n = \bigcup_{g \in G} g \cdot \Delta$; and (ii) $g \cdot \text{int}(\Delta) \cap h \cdot \text{int}(\Delta) = \emptyset$ for all
 236 $g, h \in G, g \neq h$.

237 The fundamental domain of a group G therefore provides a periodic tiling of \mathbb{R}^n by acting on Δ .
 238 This is very useful in the context of numerical sampling for neural networks which are invariant
 239 under some symmetry, since it means we can sample from a smaller subset of the input domain with
 240 a guarantee to find all the linear regions in the limit. This allows us, in principle, to be able to use far
 241 fewer samples while maintaining the same density of points.

242 **Theorem 4.3.** Let $f : \mathbb{R}^N \rightarrow \mathbb{R}$ be a tropical rational map invariant under group G . Let $\Delta \subseteq \mathbb{R}^N$ be
 243 a fundamental domain of G . Suppose \mathcal{L} is the set of linear regions. Define the following two sets

$$\begin{aligned} \mathcal{U}_c &:= \{A \in \mathcal{U} : A \subseteq \Delta\} \\ \mathcal{U}_n &:= \{A \in \mathcal{U} : A \cap \Delta \neq \emptyset\}. \end{aligned}$$

244 Then

$$|G||\mathcal{U}_c| \leq |\mathcal{U}| \leq |G||\mathcal{U}_c| + \sum_{A \in \mathcal{U}_n \setminus \mathcal{U}_c} \frac{|G|}{|G_A|}.$$

245 where $|G_A|$ is the size of the stabilizer of A .

246 This gives us a method for estimating the total number of linear regions from sampling in the
 247 fundamental domain using *multiplicity*, which we discuss next.

248 **4.2 Sampling from the Fundamental Domain**

249 To demonstrate the potential performance improvements in numerical sampling exploiting symmetry
 250 in the network architecture, we consider permutation invariant neural networks inspired by deep sets
 251 [19]. Our numerical sampling approach is inspired by very recent work in this area [20].

252 **Lemma 4.4** ([19]). *An $m \times m$ matrix W acting as a linear operator of the form $W = \lambda I_{m \times m} +$
 253 $\gamma(\mathbf{1}^T \mathbf{1})$, where $\lambda, \gamma \in \mathbb{R}$ is permutation equivariant, meaning $WPx = PWx$ for any $x \in \mathbb{R}^m$, so it
 254 commutes with any permutation matrix.*

255 Using a weight matrix of this form, we can construct permutation invariant neural networks by setting
 256 the bias to 0, applying a ReLU activation after multiplication by W , and then summing. In this case,
 257 the network is invariant under the group action S_n , so the fundamental domain is the set of points
 258 with increasing coordinates, i.e., $\Delta = \{(x_1, \dots, x_n) : x_1 \geq x_2 \geq \dots \geq x_n\}$. This splits \mathbb{R}^n into $n!$
 259 tiles, so we have a clear and significant advantage in restricting sampling to the fundamental domain.

260 Note, however, that it is important to address the multiplicities of symmetric linear regions correctly:
 261 If a given Jacobian of shape $n \times 1$ has no repeated elements, this means it is contained in the interior
 262 of some group action applied to the fundamental domain. This means there are $n!$ total linear regions
 263 with this Jacobian. If, on the other hand, there are repeated coefficients in a given Jacobian J , we
 264 consider the set $C(J)$ of counts of repeated elements. For example, for $J = [1, 1, 0]$, $C(J) = (2, 1)$.
 265 Then the multiplicity of a given Jacobian is given by

$$\text{mult}(J) = \frac{n!}{\prod_{c \in C(J)} c!}.$$

266 Using this multiplicity calculation we can efficiently estimate the number of linear regions while
 267 reducing the number of point samples by a factor of $n!$. This provides a dramatic gain in sampling
 268 efficiency.

269 In Figure 1, we present the results when Algorithm 2 is run with $R = 10, N = 10, M = 50$. These
 270 results show that the fundamental domain estimate performs well for low dimensional inputs but
 271 appears to overcount linear regions as n increases. Despite divergence, there is still utility in this
 272 metric because we are often more concerned with obtaining an upper bound on the expressivity of a
 273 neural network than an exact figure and the fundamental domain estimate does not undercount the
 274 number of linear regions.

275 **5 Symbolic Neural Networks**

276 Here, we present the details on our practical contribution of a symbolic representation of neural
 277 networks as a new library integrated into OSCAR [15].

278 **5.1 Computing Linear Regions of Tropical Puiseux Rational Maps**

279 We present an algorithm that can compute the linear regions of *any* tropical Puiseux rational function.
 280 Intuitively, we do this by computing the linear regions of the numerator and denominator, and then
 281 considering intersections of such regions and how they fit together. Thus, a first step is to understand
 282 how the computation of linear regions works for tropical Puiseux polynomials. The key to our
 283 approach will be to exploit the polyhedral connection of tropical geometry and recast the problem
 284 in the language of polyhedral geometry. This, among other things, will allow us to make use the
 285 extensive polyhedral geometry library in OSCAR [15] for implementation.

286 One important upshot from this study is that there is a strong connection between the number of
 287 linear regions of a tropical Puiseux rational function and the number of monomials that appear in
 288 its algebraic expression. Note, however, that the two are independent, in the sense that two Puiseux
 289 rational functions could have the same number of linear regions but different numbers of (nonzero)
 290 monomials, and conversely, the same number of monomials and a different number of linear regions.
 291 For instance, computing the number of linear regions requires some combinatorial data about the
 292 intersections of the polyhedra defined by monomials.

293 First, we need to know how to compute the linear regions of tropical polynomials. Let $P =$
 294 $\bigoplus_n a_n \odot x^n$ where by x^n we mean $x_1^{n_1} \odot \dots \odot x_k^{n_k}$ and powers are taken in the tropical sense. Then

295 as function $\mathbb{R}^k \rightarrow \mathbb{R}$, P is given by $\max_n \{a_n + n_1x_1 \cdots + n_kx_k\}$. It follows that the linear regions
 296 of P are precisely the sets of the form

$$S_n = \{x \in \mathbb{R}^n \mid a_m + m_1x_1 \cdots + m_kx_k \leq a_n + n_1x_1 \cdots + n_kx_k \text{ for all } m \neq n\}.$$

297 For any set U on which P is linear, we write $L(P, U)$ for the corresponding linear map. This gives us

$$L(P, S_n)(x) = a_n + n_1x_1 \cdots + n_kx_k. \quad (11)$$

298 We now rewrite (11) using polyhedral geometry. Recall that a polyhedron in \mathbb{R}^k is a set of the form
 299 $P(A, b) = \{x \in \mathbb{R}^k \mid Ax \leq b\}$. We claim that each linear region is a polyhedron: For a fixed index
 300 n , define the matrix A_n to be the $(N - 1) \times k$ matrix whose rows are the vectors $m - n$, where m
 301 ranges over the support of the coefficients of P (ordered lexicographically) and b_n to be the vector
 302 with entries $a_n - a_m$. Then $S_n = P(A_n, b_n)$. This gives us a way to encode the computation of the
 303 linear regions of tropical Puiseux polynomials using polyhedral geometry. As a direct consequence,
 304 intersections of linear regions of tropical Puiseux polynomials are also polyhedra. In particular, there
 305 are algorithms from polyhedral geometry for determining whether such polyhedra are realizable. One
 306 of the key observations given by our algorithm is that the linear regions of tropical Puiseux rational
 307 maps are *almost* given by k -dimensional intersections of the linear regions of the numerator and
 308 the denominator. Indeed, note that if U is a linear region of p and V a linear region of q , then we
 309 have $L(U \cap V, p \otimes q) = L(U, p) - L(V, q)$. The only issue that arises is that there might be some
 310 repetition in the $L(U \cap V, p \otimes q)$ as U ranges over the linear regions of p and V over the linear regions
 311 of q . In particular, linear regions of $p \otimes q$ might end up corresponding to unions of such $U \cap V$.

312 5.2 Computing Linear Regions

313 Determining the linear regions of a neural network may be approached *numerically* or *symbolically*.
 314 The numerical approach exploits the fact that linear regions of a neural network correspond to regions
 315 where the gradient is constant. Thus, to estimate the number of linear regions, we can evaluate the
 316 gradient on a sample of points (e.g., a mesh) in some large box $[-R, R]^n$. For sufficiently large R
 317 and a sufficiently dense sample of points, we get an accurate estimate. The symbolic approach, on
 318 the other hand, exploits the connection between neural networks and tropical Puiseux rational maps.
 319 Indeed, we can symbolically compute a Puiseux rational map that represents the neural network and
 320 then compute the number of linear regions using the approach outlined in section 5.1.

321 To compare each method, we ran the computations on smaller networks with varying sizes to compare
 322 run times and precision. For the symbolic approach, we generate 20 neural networks with random
 323 weights for each architecture and then compute the tropical Puiseux rational function associated to
 324 each neural network and compute the linear regions using Algorithm 3.

325 For the numerical approach, we also work with synthetic data and generate 1000 neural networks
 326 with random weights for each architecture. We then estimate the number of linear regions in a box of
 327 size $[-10, 10]^n$ and sample 1000 points from this domain.

328 In both cases, we use He initialization for the weights, i.e., we generate weights with distribution
 329 $N(0, \frac{2}{\sqrt{d}})$ where d is the input dimension. The data we obtain in this manner is summarized in Tables
 330 10 and 11. For the symbolic approach, we also track the number of nonzero monomials to compare
 331 this quantity with the number of linear regions. For networks with 3 layers, we find the numerical
 332 estimate to be quite close, but for 4 it seems to diverge. This could be because in the numerical
 333 approach, we are only counting the number of unique Jacobians that can be found in the domain. A
 334 situation could arise where the same linear function is disconnected and hence counted twice by the
 335 symbolic approach but only once for the numerical approach.

336 The main observations from our experimental study are as follows. The numerical approach is faster,
 337 but offers no guarantee of precision: When running the computation for a given R and mesh grid,
 338 there seems to be no easy way of determining whether we have indeed hit all the linear regions or
 339 whether we have obtained an accurate estimate of the arrangements of these regions. It is possible
 340 to either overestimate or underestimate the number of linear regions. In particular, there is a priori
 341 no obvious way to select the parameters. We found the symbolic approach to be more precise, but
 342 slower. In general, the number of monomials seems to be far larger than the number of linear regions,
 343 which contradicts the intuition of Figure 2.

344 Both algorithms suffer from the curse of dimensionality: in the case of the numerical approach, the
 345 number of samples in a meshgrid grows exponentially with respect to the dimension. In the case of

346 the symbolic approach, calculations with polytopes seem to scale poorly with dimension and with the
347 complexity of the neural network.

348 **6 Discussion: Limitations & Directions for Future Research**

349 In this paper, we set up a framework to interpret and analyzed the expressivity of neural networks
350 using techniques from polyhedral and tropical geometry. We demonstrated several ways in which a
351 symbolic interpretation can often enable computational optimizations for otherwise intractable tasks
352 and provided new insights into the inner workings of these networks. To the best of our knowledge,
353 ours is the first work to provide practical tropical geometric theory and algorithms to numerically
354 compute and analyze the expressivity of a neural network both in terms of inherent neural network
355 quantities as well as tropical geometric quantities.

356 Despite the theoretical and practical advancement of tropical deep learning that our work offers, it
357 is nevertheless subject to limitations, which we now discuss and which inspire directions for future
358 research.

359 **Experimental Limitations.** The curse of dimensionality is a common theme in deep learning, and
360 our work is unfortunately no exception. The methods introduced in this paper are quite fast for small
361 enough networks, but scale poorly with dimension and more complex architectures.

362 We note that the main computational bottlenecks of the Puiseux rational function associated with a
363 neural network are the implementation of fast multivariate Puiseux series operations. Our current
364 computations rely on a custom implementation of this type of operation, and one potential avenue for
365 improvement would be using such methods once they have been implemented in OSCAR [15].

366 For the computation of linear regions, both the numerical and symbolic approaches suffer from the
367 curse of dimensionality. For instance, the numerical approach requires sampling on a mesh grid in a
368 box of the form $[-R, R]^n$ where n is the input dimension. In particular, the number of points needed
369 is proportional to the volume, which scales exponentially in n . Similarly, the symbolic approach relies
370 on the computation of the Puiseux rational function associated with a neural network and polytope
371 computations, both of which are challenging computational problems in higher dimensions.

372 Most of our computations rely on carrying out some elementary computations many times. Thus,
373 another avenue of improvement for this would be to parallelize.

374 **Structural Limitations.** Much of what we are studying are basically framed as a combinatorial
375 optimization problem, which are known to be difficult. In particular, computing the Hoffman constant
376 is equivalent to the Stewart–Todd condition measure of a matrix and both quantities are NP-hard to
377 compute in general cases [17, 21].

378 Further studying and understanding where and how symbolic computation algorithms can be made
379 more efficient, e.g., by parallelization, would make our proposed approaches more applicable to
380 larger neural networks. Our work effectively proposes a new intersection of symbolic computation
381 and deep learning, so there remains infrastructure to set up to make methods from these two fields
382 compatible.

383 **References**

- 384 [1] Grigory Mikhalkin and Johannes Rau. *Tropical geometry*, volume 8. MPI for Mathematics,
385 2009.
- 386 [2] David Speyer and Bernd Sturmfels. Tropical Mathematics. *Mathematics Magazine*, 82(3):163–
387 173, 2009.
- 388 [3] Diane Maclagan and Bernd Sturmfels. *Introduction to tropical geometry*, volume 161. American
389 Mathematical Society, 2021.
- 390 [4] Razvan Pascanu, Guido Montufar, and Yoshua Bengio. On the number of response regions of
391 deep feed forward networks with piece-wise linear activations. *arXiv preprint arXiv:1312.6098*,
392 2013.

- 393 [5] Guido F Montúfar, Razvan Pascanu, Kyunghyun Cho, and Yoshua Bengio. On the number of
394 linear regions of deep neural networks. *Advances in neural information processing systems*, 27,
395 2014.
- 396 [6] Raman Arora, Amitabh Basu, Poorya Mianjy, and Anirbit Mukherjee. Understanding deep
397 neural networks with rectified linear units. *arXiv preprint arXiv:1611.01491*, 2016.
- 398 [7] Maithra Raghu, Ben Poole, Jon Kleinberg, Surya Ganguli, and Jascha Sohl-Dickstein. On the
399 expressive power of deep neural networks. In *international conference on machine learning*,
400 pages 2847–2854. PMLR, 2017.
- 401 [8] Boris Hanin and David Rolnick. Deep ReLU Networks Have Surprisingly Few Activation
402 Patterns. *Advances in neural information processing systems*, 32, 2019.
- 403 [9] Huan Xiong, Lei Huang, Mengyang Yu, Li Liu, Fan Zhu, and Ling Shao. On the number
404 of linear regions of convolutional neural networks. In *International Conference on Machine*
405 *Learning*, pages 10514–10523. PMLR, 2020.
- 406 [10] Alexis Goujon, Arian Etemadi, and Michael Unser. On the number of regions of piecewise
407 linear neural networks. *Journal of Computational and Applied Mathematics*, 441:115667, 2024.
- 408 [11] Liwen Zhang, Gregory Naitzat, and Lek-Heng Lim. Tropical geometry of deep neural networks.
409 In *International Conference on Machine Learning*, pages 5824–5832. PMLR, 2018.
- 410 [12] Vasileios Charisopoulos and Petros Maragos. A tropical approach to neural networks with
411 piecewise linear activations. *arXiv preprint arXiv:1805.08749*, 2018.
- 412 [13] Ruriko Yoshida, Georgios Aliatimis, and Keiji Miura. Tropical neural networks and its applica-
413 tions to classifying phylogenetic trees. *arXiv preprint arXiv:2309.13410*, 2023.
- 414 [14] Kurt Pasque, Christopher Teska, Ruriko Yoshida, Keiji Miura, and Jefferson Huang. Tropical
415 decision boundaries for neural networks are robust against adversarial attacks. *arXiv preprint*
416 *arXiv:2402.00576*, 2024.
- 417 [15] Oscar – open source computer algebra research system, version 1.0.0, 2024.
- 418 [16] Alan J Hoffman. On approximate solutions of systems of linear inequalities. In *Selected Papers*
419 *Of Alan J Hoffman: With Commentary*, pages 174–176. World Scientific, 2003.
- 420 [17] Javier Pena, Juan Vera, and Luis Zuluaga. An algorithm to compute the hoffman constant of a
421 system of linear constraints. *arXiv preprint arXiv:1804.08418*, 2018.
- 422 [18] Osman Güler, Alan J Hoffman, and Uriel G Rothblum. Approximations to solutions to systems
423 of linear inequalities. *SIAM Journal on Matrix Analysis and Applications*, 16(2):688–696, 1995.
- 424 [19] Manzil Zaheer, Satwik Kottur, Siamak Ravanbakhsh, Barnabas Poczos, Russ R Salakhutdinov,
425 and Alexander J Smola. Deep sets. *Advances in neural information processing systems*, 30,
426 2017.
- 427 [20] Alexis Goujon, Arian Etemadi, and Michael Unser. On the number of regions of piecewise
428 linear neural networks. *Journal of Computational and Applied Mathematics*, 441:115667, 2024.
- 429 [21] Javier F Pena, Juan C Vera, and Luis F Zuluaga. Equivalence and invariance of the chi and
430 hoffman constants of a matrix. *arXiv preprint arXiv:1905.06366*, 2019.

431 A Further Experimental Details

432 We ran the final computations on NVIDIA GeForce RTX 3090 GPUs. Table 7 lists the time taken by
 433 each experiment. Given that our experiments do not include training on large datasets, the experiments
 434 are not particularly expensive from the perspective memory usage, and all the code can be run on a
 435 laptop. The detail provided in the paper correspond roughly to the amount of computational resources
 436 that were used for this work, omitting trial and testing runs.

437 B Algorithms

Algorithm 1 Lower and approximate upper bound of Hoffman constant

Require: A : an $m \times n$ matrix; B max number of iterations; ϵ threshold of testing surjectivity.

- 1: Initialize $H_L = H^U = 0$.
 - 2: **for** $i \in 1, \dots, B$ **do**
 - 3: Sample a random integer K .
 - 4: Sample a random subset J from $\{1, \dots, m\}$ of size K .
 - 5: Solve (9). Let t be the optimal value;
 - 6: **if** $t > \epsilon$ **then**
 - 7: J is surjective. Update $H_L = \max\{H_L, \frac{1}{t}\}$;
 - 8: Compute the minimal singular value of $\hat{\rho}(A_J)$;
 - 9: **if** $\hat{\rho}(A_J) > 0$ **then**
 - 10: Update $H^U = \max\{H^U, \frac{1}{\hat{\rho}(A_J)}\}$;
- return** Lower bound H_L and approximate upper bound H^U .
-

Algorithm 2 Estimation of the ratio of fundamental domain sampling to regular sampling

Require: The input dimension n , $R \in \mathbb{R}$ side length for cube centered at the origin from which the samples are taken, M number of models to use, N base number of points to sample.

- 1: **for** $m \in 1..M$ **do**
 - 2: Create a permutation invariant model σ with input dimension n .
 - 3: Sample N^n points in the cube with side length R centered at the origin. Note that the number of points in the sample grows exponentially with the input dimension n .
 - 4: Compute the Jacobian matrices of the network at each point, round to 10 decimal place to avoid numerical errors, remove duplicates, and count the number of unique Jacobians.
 - 5: Sample $\frac{N^n}{n!}$ points from the fundamental domain of \mathbb{R}^n intersected with the sampling cube.
 - 6: Compute the unique Jacobians similarly as for the regular sampling.
 - 7: Sum the multiplicities of each Jacobian to get an estimate of the total number of linear regions.
 - 8: Record the ratio of the fundamental domain estimate to the regular estimate.
- return** The average ratio across M models.
-

438 C Proofs

439 C.1 Proof of Proposition 3.4

440 *Proof.* The polyhedra defined by

$$\left(\begin{bmatrix} A_p \\ A_q \end{bmatrix} - \mathbf{1} \begin{bmatrix} a_{i_p} \\ a_{j_q} \end{bmatrix} \right) x \leq \begin{bmatrix} b_{i_p} \mathbf{1} - b_p \\ b_{j_q} \mathbf{1} - b_q \end{bmatrix}$$

441 form a convex refinement of linear regions of f . Let

$$\text{res}_{i_p, j_q}(x) := \left(\begin{bmatrix} A_p \\ A_q \end{bmatrix} - \mathbf{1} \begin{bmatrix} a_{i_p} \\ a_{j_q} \end{bmatrix} \right) x - \begin{bmatrix} b_{i_p} \mathbf{1} - b_p \\ b_{j_q} \mathbf{1} - b_q \end{bmatrix}$$

442 denote the residual of x to the polyhedron. We have

$$R_f(x) \leq H(p \otimes q) \max\{\|\text{res}_{i_p, j_q}(x)_+\|_\infty : 1 \leq i_p \leq m_p; 1 \leq j_q \leq m_q\}.$$

Algorithm 3 Linear regions of tropical Puiseux rational functions

Require: Tropical Puiseux polynomials p, q in n variables.

- 1: Compute the linear regions U_1, \dots, U_l of p , and set $L_i = L(p, U_i)$.
- 2: Compute the linear regions V_1, \dots, V_m of q , and set $S_j = L(q, V_j)$.
- 3: Compute the pairs (i, j) such that $U_i \cap V_j$ has dimension n
- 4: **for** (i, j) such that $U_i \cap V_j$ has dimension n **do**
- 5: Compute the linear map $T_{ij} = L_i - S_j$
- 6: Set S to be the set of all T_{ij}
- 7: **for** $T \in S$ **do**
- 8: Compute the set $I(T)$ indices (i, j) such that $T = T_{ij}$.
- 9: Compute the set $C(T)$ of connected components of

$$\bigcup_{(i,j) \in I(T)} U_i \cap V_j$$

return $\bigcup_{T \in S} C(T)$.

Algorithm 4 Numerical estimation of neural network linear regions

Require: The architecture of a linear activation neural network σ with scalar output, $R \in \mathbb{R}$ side length for cube centered at the origin from which the samples are taken, M number of models to use, N number of points to sample.

- 1: **for** $m \in 1..M$ **do**
 - 2: Create a model with architecture σ and initialise weights and biases using He inialisation.
 - 3: Sample N points in the cube with side length R centered at the origin.
 - 4: Compute the Jacobian matrices of the network at each point.
 - 5: Round the Jacobians matrices to 5 decimal places to avoid floating point errors.
 - 6: Remove duplicates and count the number of unique Jacobians.
- return** The average number of linear regions.
-

443 Note that

$$\begin{aligned} \|\text{res}_{i_p, j_q}(x)_+\|_\infty &= \left\| \left(\begin{bmatrix} A_p x + b_p - \mathbf{1}(a_{i_p} x + b_{i_p}) \\ A_q x + b_q - \mathbf{1}(a_{j_q} x + b_{j_q}) \end{bmatrix} \right)_+ \right\|_\infty \\ &= \max_{k, \ell} \{ (A_p x + b_p)_k - (a_{i_p} x + b_{i_p}), (A_q x + b_q)_\ell - (a_{j_q} x + b_{j_q}), 0 \} \\ &= \max \{ p(x) - (a_{i_p} x + b_{i_p}), q(x) - (a_{j_q} x + b_{j_q}), 0 \} \end{aligned}$$

444 Therefore,

$$\begin{aligned} \max_{i_p, j_q} \|\text{res}_{i_p, j_q}(x)\|_\infty &= \max_{i_p, j_q} \{ p(x) - (a_{i_p} x + b_{i_p}), q(x) - (a_{j_q} x + b_{j_q}), 0 \} \\ &= \max \{ p(x) - \min_{i_p} \{ a_{i_p} x + b_{i_p} \}, q(x) - \min_{j_q} \{ a_{j_q} x + b_{j_q} \}, 0 \} \\ &= \max \{ p(x) - \check{p}(x), q(x) - \check{q}(x) \} \end{aligned}$$

445 which proves (6). □

446 C.2 Proof of Lemma 3.3

447 *Proof.* From the definition of minimal effective radius we have

$$\begin{aligned} R_f(x) &= \min \{ r : B(x, r) \cap U_i \neq \emptyset, U_i \in \mathcal{U} \} = \min \{ r : d(x, U_i) \leq r, U_i \in \mathcal{U} \} \\ &= \max \{ d(x, U_i) : U_i \in \mathcal{U} \}. \end{aligned}$$

448 For each linear region U_i characterized by $\tilde{A}_{U_i} x \leq \tilde{b}_{U_i}$, by (1), $d(x, U_i) \leq H(\tilde{A}_{U_i}) \|(\tilde{A}_{U_i} x - \tilde{b}_{U_i})_+\|$.
 449 Passing to maximum we have

$$R_f(x) = \max_{U_i \in \mathcal{U}} d(x, U_i) \leq \max_{U_i \in \mathcal{U}} H(\tilde{A}_{U_i}) \max_{U_i \in \mathcal{U}} \|(\tilde{A}_{U_i} x - \tilde{b}_{U_i})_+\| = H(f) \max_{U_i \in \mathcal{U}} \|(\tilde{A}_{U_i} x - \tilde{b}_{U_i})_+\|.$$

450 □

| | | | | | | | | |
|--------------------|--------|--------|--------|--------|--------|--------|--------|--------|
| Lower bounds H_L | 0.5460 | 0.1520 | 0.6220 | 0.5771 | 0.1208 | 0.0844 | 1.0389 | 0.1492 |
| Time t_L | 0.2495 | 0.2449 | 0.2446 | 0.2458 | 0.2443 | 0.2463 | 0.2466 | 0.2477 |
| True values H | 0.3298 | 0.7980 | 0.3772 | 0.8376 | 6.5934 | 2.6744 | 0.9372 | 1.2645 |
| Time t | 0.2132 | 0.1504 | 0.1253 | 0.1722 | 0.1566 | 0.1529 | 0.1721 | 0.1568 |
| Upper bounds H^U | 0.2081 | 0.5090 | 0.2903 | 1.0539 | 3.8508 | 1.3942 | 0.5484 | 0.8031 |
| Time t^U | 0.0043 | 0.0040 | 0.0040 | 0.0040 | 0.0040 | 0.0040 | 0.0040 | 0.0040 |

Table 1: Hoffman constants, lower bounds, approximate upper bounds, and their corresponding computational time for $m_p = 10$, $m_q = 5$ and $n = 3$

451 C.3 Proof of Theorem 4.3

452 *Proof.* The action of G partitions \mathcal{U} into a set of orbits $[A]$ and we have $|\mathcal{U}| = \sum_{[A] \in [\mathcal{U}]} |[A]|$.

From property (i) defining a fundamental domain $\cup_{A \in \mathcal{U}} A = \cup_{\sigma \in G} \sigma \cdot \Delta$, we have the trivial lower bound on the number of linear regions $|\mathcal{U}| \geq \sum_{A \in \mathcal{U}_c} |[A]| = |G||\mathcal{U}_c|$. Let $A \in \mathcal{U}$. By Lagrange's theorem, the orbit of A is such that $|[A]||G_A| = |G|$. Thus we have

$$|\mathcal{U}| \leq \sum_{A \in \mathcal{U}_n} |[A]| \leq |G||\mathcal{U}_c| + \sum_{A \in \mathcal{U}_n \setminus \mathcal{U}_c} \frac{|G|}{|G_A|}.$$

453

□

454 D Numerical Calculations of the Hoffman Constant

455 We illustrate the computation of Hoffman constant of tropical Puiseux rational map on synthetic data.
456 We generate tropical Puiseux rational maps by randomly generating two tropical Puiseux polynomials
457 p and q . Specifically, suppose p has m_p monomials and q has m_q monomials. We construct an
458 $m_p \times n$ matrix A_p and an $m_q \times n$ matrix A_q by uniformly sampling entries from $[0, 1]$. We then form
459 the matrix defined by (4). We then compute the exact Hoffman constant using the PVZ algorithm and
460 estimate its lower bound and approximate its upper bound by our proposed algorithm. We record the
461 computation time and the number of calls to solve the LP problem in the whole loop.

462 In the experiment we take different values of m_p , m_q , n and B . For each of the parameters we
463 repeat all computation for 8 times. The true Hoffman constants, lower bounds, upper bounds, and
464 the computation time per linear region can be found in Table 1,2,3, and the number of iterations of
465 the PVZ algorithm and average time to solve LP during each iteration can be found in Table 4,5,6.
466 From the tables we can see that computing the true Hoffman constants requires testing surjectivity
467 and solving over thousands LP problems, which costs a lot of time. Although the lower bounds and
468 approximate upper bounds can be loose, the computational time is much faster for lower bounds and
469 upper bounds, which implies its potential to apply for real data applications.

470 E Tables

471 Tables 8 and 9 summarise the outcomes of the experiments on the computation of linear regions for
472 tropical Puiseux rational functions. For a fixed number of variables n_{var} and number of monomials
473 $n_{\text{monomials}}$, we generate n_{samples} random Puiseux rational functions by picking random coefficients
474 and exponents using Julia's inbuilt random number generation functions, where both the numerator
475 and the denominator have $n_{\text{monomials}}$ monomials. We then compute the number of linear regions for
476 each of these rational functions and take the average over our all the samples that were generated.

477 F Figures

| | | | | | | | | |
|--------------------|---------|----------|----------|---------|----------|----------|---------|---------|
| Lower bounds H_L | 2.4965 | 5.9002 | 2.3501 | 3.7049 | 1.1434 | 0.8335 | 1.6517 | 2.2396 |
| Time t_L | 0.8924 | 0.9101 | 0.9127 | 0.8914 | 0.9132 | 0.9154 | 1.1117 | 0.6190 |
| True values H | 26.2231 | 726.8115 | 173.0057 | 23.8868 | 52.6080 | 8.1573 | 8.5050 | 18.7593 |
| Time t | 6.0048 | 2.3452 | 5.5451 | 3.6778 | 3.2828 | 2.9109 | 3.5494 | 1.7530 |
| Upper bounds H^U | 8.2854 | 323.5149 | 21.3290 | 7.4338 | 183.8179 | 254.1373 | 36.7961 | 32.5276 |
| Time t^U | 0.0136 | 0.0137 | 0.0143 | 0.0132 | 0.0120 | 0.0139 | 0.0148 | 0.0097 |

Table 2: Hoffman constants, lower bounds, approximate upper bounds, and their corresponding computational time for $m_p = 15$, $m_q = 9$ and $n = 6$

| | | | | | | | | |
|--------------------|---------|--------|--------|---------|---------|--------|---------|--------|
| Lower bounds H_L | 0.1120 | 0.1382 | 0.1227 | 63.9169 | 0.2331 | 0.1191 | 0.0571 | 0.1126 |
| Time t_L | 0.2622 | 0.2628 | 0.2625 | 0.2672 | 0.2771 | 0.2715 | 0.2689 | 0.2633 |
| True values H | 0.0017 | 1.2683 | 1.5375 | 0.0832 | 0.2777 | 0.3537 | 0.0464 | 0.1586 |
| Time t | 0.0112 | 0.0217 | 0.1002 | 0.0182 | 0.0582 | 0.0693 | 0.0189 | 0.0122 |
| Upper bounds H^U | 10.6826 | 1.7551 | 3.2794 | 7.2134 | 26.4648 | 2.6868 | 25.0251 | 5.1308 |
| Time t^U | 0.0775 | 0.0789 | 0.0780 | 0.0784 | 0.0789 | 0.0782 | 0.0782 | 0.0769 |

Table 3: Hoffman constants, lower bounds, approximate upper bounds, and their corresponding computational time for $m_p = 15$, $m_q = 5$ and $n = 7$

| | | | | | | | | |
|--------------|--------|--------|--------|--------|--------|--------|--------|--------|
| # iterations | 94 | 86 | 67 | 83 | 99 | 86 | 75 | 83 |
| Time per LP | 0.0042 | 0.0026 | 0.0025 | 0.0026 | 0.0025 | 0.0025 | 0.0026 | 0.0026 |

Table 4: Number of iterations in the PVZ algorithm and average time to solve LP during each iteration for $m_p = 10$, $m_q = 5$ and $n = 3$

| | | | | | | | | |
|--------------|--------|--------|--------|--------|--------|--------|--------|--------|
| # iterations | 2437 | 1110 | 1731 | 1441 | 1432 | 1706 | 1741 | 1095 |
| Time per LP | 0.0152 | 0.0093 | 0.0092 | 0.0098 | 0.0098 | 0.0102 | 0.0095 | 0.0097 |

Table 5: Number of iterations in the PVZ algorithm and average time to solve LP during each iteration for $m_p = 15$, $m_q = 9$ and $n = 6$

| | | | | | | | | |
|--------------|--------|--------|--------|--------|--------|--------|--------|--------|
| # iterations | 2 | 607 | 525 | 80 | 194 | 355 | 78 | 19 |
| Time per LP | 0.0027 | 0.0027 | 0.0026 | 0.0027 | 0.0032 | 0.0027 | 0.0028 | 0.0027 |

Table 6: Number of iterations in the PVZ algorithm and average time to solve LP during each iteration for $m_p = 15$, $m_q = 5$ and $n = 7$

| | |
|---|--------------|
| Experiment | Compute time |
| Linear regions of tropical Puiseux rational functions (3 variables) | 4.7 hours |
| Linear regions of tropical Puiseux rational functions (4 variables) | 13.3 hours |
| Symbolic linear regions computation for neural networks | 35 minutes |
| Numeric linear regions computation for neural networks | 4.9 minutes |
| Sampling on fundamental domain | 13 minutes |

Table 7: Compute details

| | | |
|------------------------|---------------------------|-----------------|
| $n_{\text{monomials}}$ | Average number of regions | Average runtime |
| 20 | 84.4 | 4.0 seconds |
| 50 | 160.1 | 11.6 seconds |
| 100 | 264.2 | 29.5 seconds |
| 200 | 375.2 | 66.0 seconds |
| 350 | 500.8 | 139.2 seconds |
| 500 | 580.8 | 202.7 seconds |
| 800 | 706.1 | 394.8 seconds |
| 1000 | 776.2 | 563.6 seconds |

Table 8: Computation for $n_{\text{var}} = 3$, $n_{\text{samples}} = 12$

| $n_{\text{monomials}}$ | Average number of regions | Average runtime |
|------------------------|---------------------------|-----------------|
| 20 | 157.5 | 12.6 seconds |
| 50 | 398.75 | 50.3 seconds |
| 100 | 667.75 | 83.8 seconds |
| 200 | 1021.5 | 237.5 seconds |
| 350 | 1614.5 | 987.3 seconds |
| 500 | 1909.5 | 1682.1 seconds |
| 800 | 2432.0 | 3436.7 seconds |
| 1000 | 2876.5 | 5441.8 seconds |

Table 9: Computation for $n_{\text{var}} = 4$, $n_{\text{samples}} = 4$

| Architecture | Average number of linear regions | Average number of monomials | Average runtime(s) |
|--------------|----------------------------------|-----------------------------|--------------------|
| [2, 2, 1] | 3.85 | 5.75 | 0.4166 |
| [4, 3, 1] | 6.75 | 9 | 0.4646 |
| [4, 4, 1] | 14.2 | 13.55 | 1.5794 |
| [3, 2, 2, 1] | 6.8 | 30.15 | 1.7679 |
| [3, 3, 2, 1] | 17.55 | 176.75 | 97.9659 |

Table 10: Symbolic computation

| Architecture | Average number of linear regions | Average runtime(s) |
|--------------|----------------------------------|--------------------|
| [2, 2, 1] | 3.041 | 0.01667 |
| [4, 3, 1] | 6.339 | 0.01667 |
| [4, 4, 1] | 11.936 | 0.01667 |
| [3, 2, 2, 1] | 3.549 | 0.01683 |
| [3, 3, 2, 1] | 7.381 | 0.01678 |

Table 11: Numerical computation

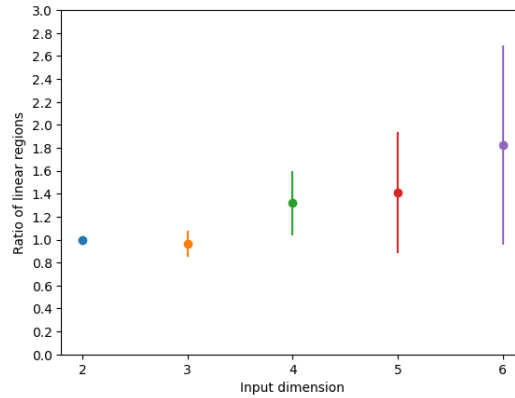


Figure 1: Ratio estimates for different input sizes with standard deviation error bars

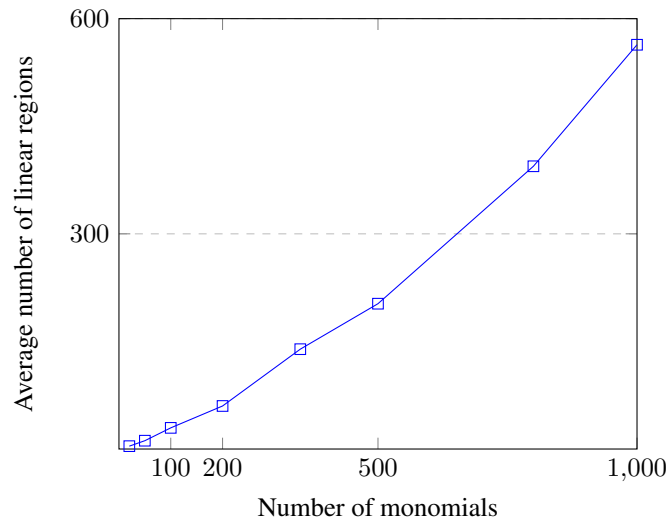


Figure 2: Linear regions of a Puiseux rational function in 3 variables

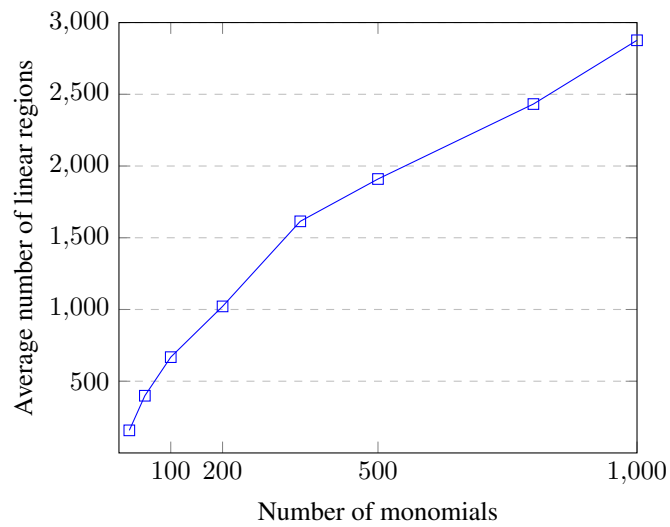


Figure 3: Linear regions of a Puiseux rational function in 4 variables

478 **NeurIPS Paper Checklist**

479 **1. Claims**

480 Question: Do the main claims made in the abstract and introduction accurately reflect the
481 paper's contributions and scope?

482 Answer: [\[Yes\]](#)

483 Justification: Each of the three contributions mentioned in the abstract has a whole section
484 devoted to it, including theoretical results and experiments. We also provided an in-depth
485 discussion of the limitations of our work in Section 6.

486 Guidelines:

- 487 • The answer NA means that the abstract and introduction do not include the claims
488 made in the paper.
- 489 • The abstract and/or introduction should clearly state the claims made, including the
490 contributions made in the paper and important assumptions and limitations. A No or
491 NA answer to this question will not be perceived well by the reviewers.
- 492 • The claims made should match theoretical and experimental results, and reflect how
493 much the results can be expected to generalize to other settings.
- 494 • It is fine to include aspirational goals as motivation as long as it is clear that these goals
495 are not attained by the paper.

496 **2. Limitations**

497 Question: Does the paper discuss the limitations of the work performed by the authors?

498 Answer: [\[Yes\]](#)

499 Justification: We provided a detailed discussion of the limitations of our work, both compu-
500 tational and theoretical in Section 6.

501 Guidelines:

- 502 • The answer NA means that the paper has no limitation while the answer No means that
503 the paper has limitations, but those are not discussed in the paper.
- 504 • The authors are encouraged to create a separate "Limitations" section in their paper.
- 505 • The paper should point out any strong assumptions and how robust the results are to
506 violations of these assumptions (e.g., independence assumptions, noiseless settings,
507 model well-specification, asymptotic approximations only holding locally). The authors
508 should reflect on how these assumptions might be violated in practice and what the
509 implications would be.
- 510 • The authors should reflect on the scope of the claims made, e.g., if the approach was
511 only tested on a few datasets or with a few runs. In general, empirical results often
512 depend on implicit assumptions, which should be articulated.
- 513 • The authors should reflect on the factors that influence the performance of the approach.
514 For example, a facial recognition algorithm may perform poorly when image resolution
515 is low or images are taken in low lighting. Or a speech-to-text system might not be
516 used reliably to provide closed captions for online lectures because it fails to handle
517 technical jargon.
- 518 • The authors should discuss the computational efficiency of the proposed algorithms
519 and how they scale with dataset size.
- 520 • If applicable, the authors should discuss possible limitations of their approach to
521 address problems of privacy and fairness.
- 522 • While the authors might fear that complete honesty about limitations might be used by
523 reviewers as grounds for rejection, a worse outcome might be that reviewers discover
524 limitations that aren't acknowledged in the paper. The authors should use their best
525 judgment and recognize that individual actions in favor of transparency play an impor-
526 tant role in developing norms that preserve the integrity of the community. Reviewers
527 will be specifically instructed to not penalize honesty concerning limitations.

528 **3. Theory Assumptions and Proofs**

529 Question: For each theoretical result, does the paper provide the full set of assumptions and
530 a complete (and correct) proof?

531
532
533
534
535
536
537
538
539
540
541
542
543
544
545
546
547
548
549
550
551
552
553
554
555
556
557
558
559
560
561
562
563
564
565
566
567
568
569
570
571
572
573
574
575
576
577
578
579
580
581
582
583
584

Answer: [Yes]

Justification: We clearly define all mathematical terms and the proofs are explained in detail and are correct to the best of our knowledge.

Guidelines:

- The answer NA means that the paper does not include theoretical results.
- All the theorems, formulas, and proofs in the paper should be numbered and cross-referenced.
- All assumptions should be clearly stated or referenced in the statement of any theorems.
- The proofs can either appear in the main paper or the supplemental material, but if they appear in the supplemental material, the authors are encouraged to provide a short proof sketch to provide intuition.
- Inversely, any informal proof provided in the core of the paper should be complemented by formal proofs provided in appendix or supplemental material.
- Theorems and Lemmas that the proof relies upon should be properly referenced.

4. Experimental Result Reproducibility

Question: Does the paper fully disclose all the information needed to reproduce the main experimental results of the paper to the extent that it affects the main claims and/or conclusions of the paper (regardless of whether the code and data are provided or not)?

Answer: [Yes]

Justification: Our paper describes the algorithms that are used to run the experiments, and our submission includes all the code necessary to run these together with instructions detailing how to use it.

Guidelines:

- The answer NA means that the paper does not include experiments.
- If the paper includes experiments, a No answer to this question will not be perceived well by the reviewers: Making the paper reproducible is important, regardless of whether the code and data are provided or not.
- If the contribution is a dataset and/or model, the authors should describe the steps taken to make their results reproducible or verifiable.
- Depending on the contribution, reproducibility can be accomplished in various ways. For example, if the contribution is a novel architecture, describing the architecture fully might suffice, or if the contribution is a specific model and empirical evaluation, it may be necessary to either make it possible for others to replicate the model with the same dataset, or provide access to the model. In general, releasing code and data is often one good way to accomplish this, but reproducibility can also be provided via detailed instructions for how to replicate the results, access to a hosted model (e.g., in the case of a large language model), releasing of a model checkpoint, or other means that are appropriate to the research performed.
- While NeurIPS does not require releasing code, the conference does require all submissions to provide some reasonable avenue for reproducibility, which may depend on the nature of the contribution. For example
 - (a) If the contribution is primarily a new algorithm, the paper should make it clear how to reproduce that algorithm.
 - (b) If the contribution is primarily a new model architecture, the paper should describe the architecture clearly and fully.
 - (c) If the contribution is a new model (e.g., a large language model), then there should either be a way to access this model for reproducing the results or a way to reproduce the model (e.g., with an open-source dataset or instructions for how to construct the dataset).
 - (d) We recognize that reproducibility may be tricky in some cases, in which case authors are welcome to describe the particular way they provide for reproducibility. In the case of closed-source models, it may be that access to the model is limited in some way (e.g., to registered users), but it should be possible for other researchers to have some path to reproducing or verifying the results.

585 **5. Open access to data and code**

586 Question: Does the paper provide open access to the data and code, with sufficient instruc-
587 tions to faithfully reproduce the main experimental results, as described in supplemental
588 material?

589 Answer: [Yes]

590 Justification: We provided all the code that is necessary to reproduce the experimental
591 results, together with instructions on how to run this.

592 Guidelines:

- 593 • The answer NA means that paper does not include experiments requiring code.
- 594 • Please see the NeurIPS code and data submission guidelines ([https://nips.cc/
595 public/guides/CodeSubmissionPolicy](https://nips.cc/public/guides/CodeSubmissionPolicy)) for more details.
- 596 • While we encourage the release of code and data, we understand that this might not be
597 possible, so “No” is an acceptable answer. Papers cannot be rejected simply for not
598 including code, unless this is central to the contribution (e.g., for a new open-source
599 benchmark).
- 600 • The instructions should contain the exact command and environment needed to run to
601 reproduce the results. See the NeurIPS code and data submission guidelines ([https:
602 //nips.cc/public/guides/CodeSubmissionPolicy](https://nips.cc/public/guides/CodeSubmissionPolicy)) for more details.
- 603 • The authors should provide instructions on data access and preparation, including how
604 to access the raw data, preprocessed data, intermediate data, and generated data, etc.
- 605 • The authors should provide scripts to reproduce all experimental results for the new
606 proposed method and baselines. If only a subset of experiments are reproducible, they
607 should state which ones are omitted from the script and why.
- 608 • At submission time, to preserve anonymity, the authors should release anonymized
609 versions (if applicable).
- 610 • Providing as much information as possible in supplemental material (appended to the
611 paper) is recommended, but including URLs to data and code is permitted.

612 **6. Experimental Setting/Details**

613 Question: Does the paper specify all the training and test details (e.g., data splits, hyper-
614 parameters, how they were chosen, type of optimizer, etc.) necessary to understand the
615 results?

616 Answer: [Yes]

617 Justification: The paper gives some details about how the synthetic data used for experiments
618 was generated. Moreover, we also provide the code that is necessary to run the experiments.

619 Guidelines:

- 620 • The answer NA means that the paper does not include experiments.
- 621 • The experimental setting should be presented in the core of the paper to a level of detail
622 that is necessary to appreciate the results and make sense of them.
- 623 • The full details can be provided either with the code, in appendix, or as supplemental
624 material.

625 **7. Experiment Statistical Significance**

626 Question: Does the paper report error bars suitably and correctly defined or other appropriate
627 information about the statistical significance of the experiments?

628 Answer: [Yes]

629 Justification: Our figures clearly demonstrate error bars when appropriate and we disclose
630 the experimental setup relevant to the statistical significance of our experiments.

631 Guidelines:

- 632 • The answer NA means that the paper does not include experiments.
- 633 • The authors should answer "Yes" if the results are accompanied by error bars, confi-
634 dence intervals, or statistical significance tests, at least for the experiments that support
635 the main claims of the paper.

- 636 • The factors of variability that the error bars are capturing should be clearly stated (for
637 example, train/test split, initialization, random drawing of some parameter, or overall
638 run with given experimental conditions).
- 639 • The method for calculating the error bars should be explained (closed form formula,
640 call to a library function, bootstrap, etc.)
- 641 • The assumptions made should be given (e.g., Normally distributed errors).
- 642 • It should be clear whether the error bar is the standard deviation or the standard error
643 of the mean.
- 644 • It is OK to report 1-sigma error bars, but one should state it. The authors should
645 preferably report a 2-sigma error bar than state that they have a 96% CI, if the hypothesis
646 of Normality of errors is not verified.
- 647 • For asymmetric distributions, the authors should be careful not to show in tables or
648 figures symmetric error bars that would yield results that are out of range (e.g. negative
649 error rates).
- 650 • If error bars are reported in tables or plots, The authors should explain in the text how
651 they were calculated and reference the corresponding figures or tables in the text.

652 8. Experiments Compute Resources

653 Question: For each experiment, does the paper provide sufficient information on the com-
654 puter resources (type of compute workers, memory, time of execution) needed to reproduce
655 the experiments?

656 Answer: [Yes]

657 Justification: The appendix provides some detail on the type of compute that was used (type
658 of GPU, memory), as well as runtimes for each experiment.

659 Guidelines:

- 660 • The answer NA means that the paper does not include experiments.
- 661 • The paper should indicate the type of compute workers CPU or GPU, internal cluster,
662 or cloud provider, including relevant memory and storage.
- 663 • The paper should provide the amount of compute required for each of the individual
664 experimental runs as well as estimate the total compute.
- 665 • The paper should disclose whether the full research project required more compute
666 than the experiments reported in the paper (e.g., preliminary or failed experiments that
667 didn't make it into the paper).

668 9. Code Of Ethics

669 Question: Does the research conducted in the paper conform, in every respect, with the
670 NeurIPS Code of Ethics <https://neurips.cc/public/EthicsGuidelines?>

671 Answer: [Yes]

672 Justification: We are carefully read through the code of ethics and to the best of our
673 knowledge the contributions in this paper do not violate it in any way.

674 Guidelines:

- 675 • The answer NA means that the authors have not reviewed the NeurIPS Code of Ethics.
- 676 • If the authors answer No, they should explain the special circumstances that require a
677 deviation from the Code of Ethics.
- 678 • The authors should make sure to preserve anonymity (e.g., if there is a special consid-
679 eration due to laws or regulations in their jurisdiction).

680 10. Broader Impacts

681 Question: Does the paper discuss both potential positive societal impacts and negative
682 societal impacts of the work performed?

683 Answer: [NA]

684 Justification: The work does not have any obvious harmful applications or any potential
685 negative societal impact.

686 Guidelines:

- 687 • The answer NA means that there is no societal impact of the work performed.
- 688 • If the authors answer NA or No, they should explain why their work has no societal
- 689 impact or why the paper does not address societal impact.
- 690 • Examples of negative societal impacts include potential malicious or unintended uses
- 691 (e.g., disinformation, generating fake profiles, surveillance), fairness considerations
- 692 (e.g., deployment of technologies that could make decisions that unfairly impact specific
- 693 groups), privacy considerations, and security considerations.
- 694 • The conference expects that many papers will be foundational research and not tied
- 695 to particular applications, let alone deployments. However, if there is a direct path to
- 696 any negative applications, the authors should point it out. For example, it is legitimate
- 697 to point out that an improvement in the quality of generative models could be used to
- 698 generate deepfakes for disinformation. On the other hand, it is not needed to point out
- 699 that a generic algorithm for optimizing neural networks could enable people to train
- 700 models that generate Deepfakes faster.
- 701 • The authors should consider possible harms that could arise when the technology is
- 702 being used as intended and functioning correctly, harms that could arise when the
- 703 technology is being used as intended but gives incorrect results, and harms following
- 704 from (intentional or unintentional) misuse of the technology.
- 705 • If there are negative societal impacts, the authors could also discuss possible mitigation
- 706 strategies (e.g., gated release of models, providing defenses in addition to attacks,
- 707 mechanisms for monitoring misuse, mechanisms to monitor how a system learns from
- 708 feedback over time, improving the efficiency and accessibility of ML).

709 11. Safeguards

710 Question: Does the paper describe safeguards that have been put in place for responsible
 711 release of data or models that have a high risk for misuse (e.g., pretrained language models,
 712 image generators, or scraped datasets)?

713 Answer: [NA]

714 Justification: The work does not pose any such risks.

715 Guidelines:

- 716 • The answer NA means that the paper poses no such risks.
- 717 • Released models that have a high risk for misuse or dual-use should be released with
- 718 necessary safeguards to allow for controlled use of the model, for example by requiring
- 719 that users adhere to usage guidelines or restrictions to access the model or implementing
- 720 safety filters.
- 721 • Datasets that have been scraped from the Internet could pose safety risks. The authors
- 722 should describe how they avoided releasing unsafe images.
- 723 • We recognize that providing effective safeguards is challenging, and many papers do
- 724 not require this, but we encourage authors to take this into account and make a best
- 725 faith effort.

726 12. Licenses for existing assets

727 Question: Are the creators or original owners of assets (e.g., code, data, models), used in
 728 the paper, properly credited and are the license and terms of use explicitly mentioned and
 729 properly respected?

730 Answer: [Yes]

731 Justification: Where we have used or been inspired by previous work we have made sure
 732 that we have legal permission to use it and have clearly cited it in each case.

733 Guidelines:

- 734 • The answer NA means that the paper does not use existing assets.
- 735 • The authors should cite the original paper that produced the code package or dataset.
- 736 • The authors should state which version of the asset is used and, if possible, include a
- 737 URL.
- 738 • The name of the license (e.g., CC-BY 4.0) should be included for each asset.

- 739
- For scraped data from a particular source (e.g., website), the copyright and terms of service of that source should be provided.
 - 740
 - 741
 - 742
 - 743
 - 744
 - 745
 - 746
 - 747
 - 748

749 13. **New Assets**

750 Question: Are new assets introduced in the paper well documented and is the documentation
751 provided alongside the assets?

752 Answer: [Yes]

753 Justification: The new Julia library contains well documented code which has a clear and
754 accessible API. All our code for all experiments and applications is released under the CC
755 BY 4.0 licence.

756 Guidelines:

- 757 • The answer NA means that the paper does not release new assets.
- 758 • Researchers should communicate the details of the dataset/code/model as part of their
759 submissions via structured templates. This includes details about training, license,
760 limitations, etc.
- 761 • The paper should discuss whether and how consent was obtained from people whose
762 asset is used.
- 763 • At submission time, remember to anonymize your assets (if applicable). You can either
764 create an anonymized URL or include an anonymized zip file.

765 14. **Crowdsourcing and Research with Human Subjects**

766 Question: For crowdsourcing experiments and research with human subjects, does the paper
767 include the full text of instructions given to participants and screenshots, if applicable, as
768 well as details about compensation (if any)?

769 Answer: [NA]

770 Justification: This work did not involve crowdsourcing nor research with human subjects.

771 Guidelines:

- 772 • The answer NA means that the paper does not involve crowdsourcing nor research with
773 human subjects.
- 774 • Including this information in the supplemental material is fine, but if the main contribu-
775 tion of the paper involves human subjects, then as much detail as possible should be
776 included in the main paper.
- 777 • According to the NeurIPS Code of Ethics, workers involved in data collection, curation,
778 or other labor should be paid at least the minimum wage in the country of the data
779 collector.

780 15. **Institutional Review Board (IRB) Approvals or Equivalent for Research with Human 781 Subjects**

782 Question: Does the paper describe potential risks incurred by study participants, whether
783 such risks were disclosed to the subjects, and whether Institutional Review Board (IRB)
784 approvals (or an equivalent approval/review based on the requirements of your country or
785 institution) were obtained?

786 Answer: [NA]

787 Justification: This work did not involve crowdsourcing nor research with human subjects.

788 Guidelines:

- 789 • The answer NA means that the paper does not involve crowdsourcing nor research with
790 human subjects.

791
792
793
794
795
796
797
798

- Depending on the country in which research is conducted, IRB approval (or equivalent) may be required for any human subjects research. If you obtained IRB approval, you should clearly state this in the paper.
- We recognize that the procedures for this may vary significantly between institutions and locations, and we expect authors to adhere to the NeurIPS Code of Ethics and the guidelines for their institution.
- For initial submissions, do not include any information that would break anonymity (if applicable), such as the institution conducting the review.